

# Voltammetric behaviour of iron in cement.

## III. Comparison of iron versus reinforcing steel

J. T. HINATSU, W. F. GRAYDON, F. R. FOULKES\*

*Department of Chemical Engineering and Applied Chemistry, University of Toronto, Toronto, Ontario M5S 1A4, Canada*

Received 5 June 1990; revised 27 August 1990

The cyclic voltammetric behaviour of reinforcing steel in cured Portland cement paste was investigated and compared with that of pure iron. The cyclic voltammetric behaviour of reinforcing steel in cement is very similar to that reported earlier for iron in cement, both with and without NaCl and NaNO<sub>2</sub> (a corrosion inhibitor) additions. This similarity confirms that the results and conclusions obtained using iron are also applicable to the behaviour of reinforcing steel. A useful method for determining true surface areas of iron or steel electrodes by linear sweep voltammetry also is described in detail.

### 1. Introduction

In previous communications [1, 2], we reported the development and use of a reproducible method for cyclic voltammetric measurements on iron in cement. This voltammetric method was developed to study phenomena related to various aspects of the passivation and corrosion of reinforcing steel in concrete. Accordingly, in this study, we present results which show the similarity between the voltammetric behaviour of reinforcing steel in cement and that previously reported for iron in cement [1, 2]. This similarity further confirms the validity and applicability of the voltammetric method for studying the behaviour of steel in concrete.

A wide range of compositions is allowed for reinforcing steel, as can be seen from the compositions of the steel used in this study and by previous investigators in rebar corrosion studies [3-6], as well as from ASTM specification A706-76 for reinforcement steel, shown in Table 1. Reinforcing steel typically is made from various scrap steels; for example, the reinforcing steel used in the present study contained detectable amounts of zinc and lead (likely from galvanized steel), and chromium, nickel and molybdenum (likely from stainless steels).

On account of this wide variability in the composition of reinforcing steel, the use of iron, rather than actual reinforcing steel, was deemed to be preferable for the development of a standard voltammetric procedure [1, 2], in order to maximize the reliability of comparisons of results from different laboratories. Furthermore, the reproducible preparation of reinforcing steel electrodes in a form suitable for cyclic voltammetric measurements in cured cement is difficult. The use of iron electrodes also enables one to

attribute any interesting results to the complex cement factors, rather than to metallurgical impurities.

Fortunately, in the passive region (pH 10-13), the effects of small metallurgical factors on the corrosion of steel are minor [7] (although in acidic environments, impurities such as sulphur or phosphorus may have a detrimental effect on the corrosion resistance of steel relative to that of iron). The influence of small metallurgical differences among different reinforcing steels on their electrochemical corrosion behaviour usually is considered to be minor when compared with the influence of the complex alkaline environment of Portland cement concrete (for example, see [8]). In this work, we confirm the expected similarity of the voltammetric behaviour between iron and reinforcement steel in cured cement.

### 2. Experimental details

The cyclic voltammetric experiments were conducted according to the procedure described earlier in detail in Parts I and II [1, 2]. Briefly, the method involves embedding iron wire (Johnson-Matthey, 99.999% Fe, 0.25 mm diameter) in cement paste. The resulting iron-reinforced cement cylinders are cured for three days at 100% relative humidity. *IR*-compensated cyclic voltammograms then are run at 0.050 V s<sup>-1</sup> from -1.4 V to +0.4 V (all potentials quoted herein were measured with respect to the saturated calomel electrode (SCE)). The electrochemical cell essentially was of standard three-electrode design, except that four counter electrodes were used in order to maintain cylindrical geometry. Saturated Ca(OH)<sub>2</sub> was used as the cell electrolyte. All experiments were carried out at 25 ± 0.2°C.

In some of the experiments, sodium chloride was

\* Author to whom correspondence should be addressed.

introduced into the cement by immersing the cement electrodes in 'external solutions' of saturated  $\text{Ca}(\text{OH})_2 + \text{NaCl}$  (various concentrations) for 24 h, following the 3 day air cure, and before potential cycling. Also, sodium nitrite corrosion inhibitor was introduced into some of the samples as an admixture (i.e., dissolved in the cement mix water), as would be done in actual practice. The sodium nitrite was added by weight, as a percentage of the dry cement in the cement mix.

The reinforcing steel samples were turnings cut on a lathe from a piece of  $\frac{3}{4}$  inch diameter reinforcing rod. The spiral-shaped turnings consisted of "wire" of roughly rectangular cross-section (about  $0.1 \text{ mm} \times 0.2 \text{ mm}$ ), and were embedded in cement using essentially the same method previously described [1] for iron wire. However, whereas the iron wire samples were mechanically polished with alumina before embedding in cement, thorough polishing of the visibly rough steel turnings was impractical.

The composition of the steel was determined by combustion and DCP analysis; carbon, sulphur and nitrogen were determined by combustion in oxygen (Lico apparatus), and the other elements were determined by DCP. Samples for DCP analysis were prepared by dissolving accurately weighed steel samples in analytical grade nitric acid to give about 0.5% or 1.0% total dissolved solids. The final nitric acid concentration was about 6% by volume. A matrix blank showed no detectable metallic impurities. Similarly, results for solutions containing 0.5% or 1.0% dissolved 99.999% Fe showed that there were no interferences from the relatively large quantities of Fe in the steel samples.

### 3. Results and discussion

#### 3.1. Comparison of voltammograms for reinforcing steel and iron in cured Portland cement paste

Voltammograms for rebar turnings and iron embedded in cured Portland cement paste, using nominal current densities (i.e., current densities based on geometric electrode areas), are shown in Fig. 1. The electrochemical reactions corresponding to the various peaks have been discussed previously (see [1] and references therein). In alkaline solutions, peaks 1 and 2 usually

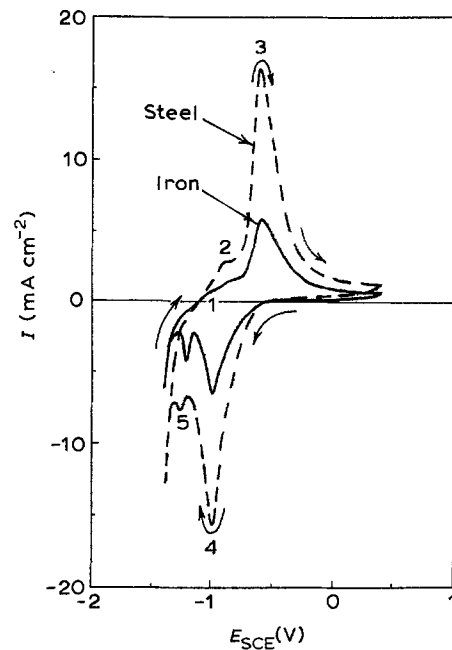


Fig. 1. Cyclic voltammograms for iron and reinforcing steel in cured Portland cement paste. Current densities are based on the geometric surface areas. Cell electrolyte was saturated  $\text{Ca}(\text{OH})_2$ , water-to-cement ratio = 0.45, 3 day cure,  $25^\circ \text{C}$ ,  $0.050 \text{ V s}^{-1}$ . Cycle number 201 shown.

are attributed to the formation of ferrous hydroxide from the base metal. Peak 3 is the passivation peak, where poorly-protective ferrous species are converted into protective ferric species (possibly  $\text{CaFe}_2\text{O}_4$  [2]). Peak 4 is the cathodic reduction peak associated with peak 3, while peak 5 is the reduction peak associated with peaks 1 and 2.

Although the shapes of the voltammograms were comparable, the nominal current densities obtained with reinforcing steel are greater than those obtained with iron at all potentials. This is not surprising, since the surface roughness of the rebar turnings was considerably greater than that of the polished iron wires, as could be clearly seen by visual examination. The independent determination of the surface areas of iron and steel electrodes therefore is of interest, since reporting of current densities based on "true" surface areas, rather than on geometric areas (from geometric measurements, assuming smooth surfaces), would provide a more representative comparison of our results for steel with our results for iron. Reporting of

Table 1. Compositions of reinforcement steel used in this study and by other workers\*

Reference	C	Mn	Si	P	S	Cr	Ni	Mo	Zn	Pb	Cu
[3]	0.20	0.50		0.057	0.07						
[4]	0.39	1.46	0.08	0.006	0.021						
[5]	0.25	1.30	0.39	0.02	0.08	0.01					
[6]	0.85	0.78	0.22	0.24	0.017						
This study	0.42	0.66	0.03	0.01	0.04	0.11	0.11	0.025	0.02	0.003	0.28
ASTM A707-76	$\leq 0.30$	$\leq 1.5$	$\leq 0.5$	$\leq 0.035$	$\leq 0.045$						

\* Compositions shown are weight percents.

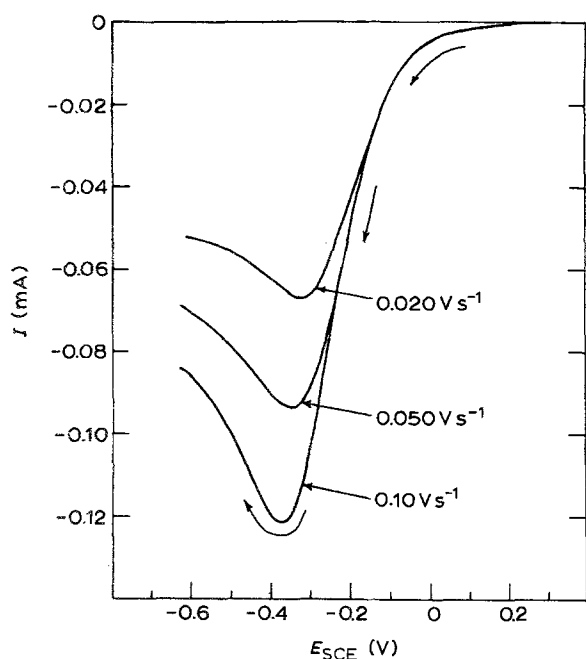
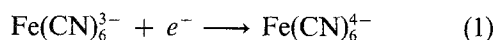


Fig. 2. Linear sweep voltammograms for iron wires in 0.010 M  $K_3FeCN_6$  + 1.0 M KOH at 25°C.

current densities based on true surface areas also facilitates the comparison of results from different workers, who may have used iron or steel electrodes having different surface roughnesses.

The true surface areas and the corresponding roughness factors (true surface area/geometric surface area) of the steel turnings and the iron wires were determined by linear sweep voltammetry (LSV), using the reaction



LSV with the ferricyanide-ferrocyanide couple is often used for the determination of true surface areas (for

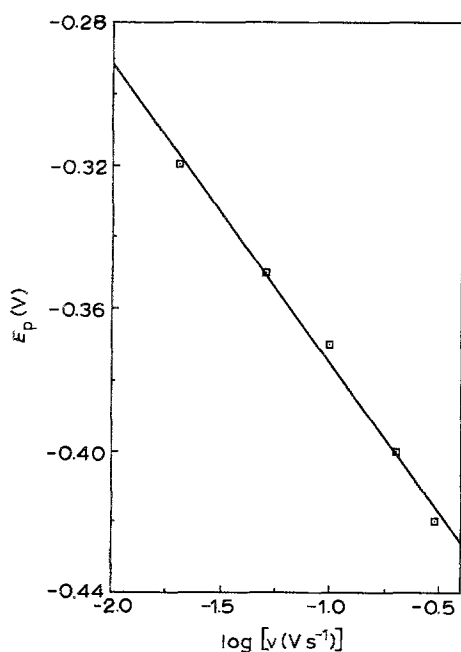


Fig. 3. Peak potentials for iron wires in 0.010 M  $K_3FeCN_6$  + 1.0 M KOH at 25°C against the logarithm of the potential sweep rate.

example, see [9]). Cathodic voltammograms (first half-cycles) obtained with iron electrodes in 10.0 mM  $K_3Fe(CN)_6$  + 1.0 M KOH are shown in Fig. 2. These cathodic potential sweeps covered a range from the rest potential of about +0.3 V to about -0.6 V. The peak potentials ( $E_p$ ) varied linearly with the logarithm of the potential sweep rate (see Fig. 3), and  $|E_p - E_{p/2}| \sim 150$  mV, which indicates an irreversible reaction with a transfer coefficient ( $\alpha$ ) of about 0.3 [10]. Thus, in order to rule out any effects of this irreversibility on the measured surface areas, potential sweeps also were run with steel and iron electrodes that had been coated with a thin layer of gold, since the cathodic reduction of ferricyanide on gold shows reversible behaviour [9]. The gold coatings were applied by vapour deposition, using a Polaron SEM Coating System. A sputtering current of 20 mA was maintained for 15 min in an atmosphere of about 0.12 torr Ar. Cathodic voltammograms (first half-cycle) obtained with gold-coated iron electrodes are shown in Fig. 4. The peak potentials did not vary with sweep rate, and  $|E_p - E_{p/2}| \sim 60$  mV, as expected for a reversible electrode reaction.

For irreversible electrode reactions [10],

$$i_p = (2.99 \times 10^5) n(n_a \alpha)^{1/2} A D^{1/2} v^{1/2} C \quad (2)$$

or

$$A = (i_p/v^{1/2}) / \{(2.99 \times 10^5) n(n_a \alpha)^{1/2} D^{1/2} C\} \quad (3)$$

where  $i_p$  is the peak current (amperes),  $n$  is the number of electrons transferred ( $n = 1$  for the ferri-ferrocyanide couple),  $n_a$  is the number of electrons transferred in the rate-determining step (taken as 1),  $A$  is the true electrode area ( $cm^2$ ),  $D$  is the diffusion coefficient for  $Fe(CN)_6^{3-}$  ( $cm^2 s^{-1}$ ),  $v$  is the potential sweep rate ( $V s^{-1}$ ) and  $C$  is the bulk concentration of  $Fe(CN)_6^{3-}$  ( $mol cm^{-3}$ ). Similarly, for reversible elec-

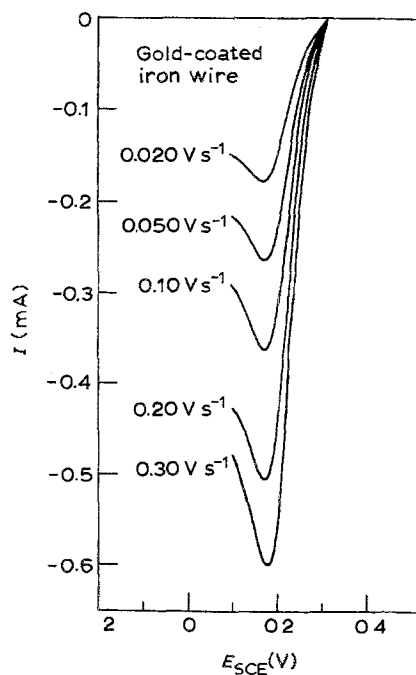


Fig. 4. Linear sweep voltammograms for gold-coated iron wires in 0.010 M  $K_3FeCN_6$  + 1.0 M KOH at 25°C.

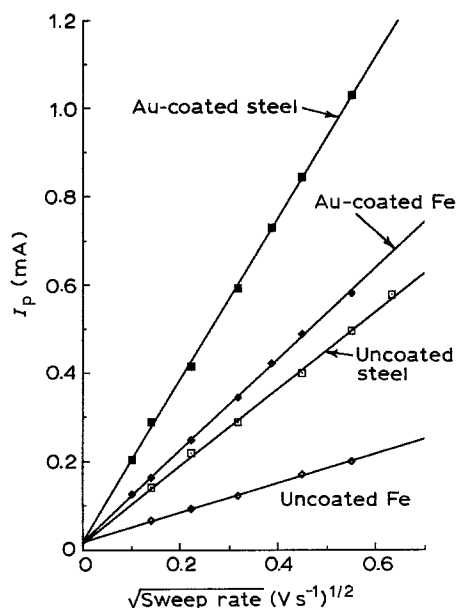


Fig. 5. Peak currents for iron wires and steel turnings in 0.010 M  $K_3FeCN_6 + 1.0M$  KOH against the square root of the potential sweep rate at 25°C. (Electrodes were of different geometric areas.)

trode reactions [10]

$$A = (i_p/v^{1/2})/\{(2.69 \times 10^5)n^{3/2}D^{1/2}C\} \quad (4)$$

Thus, the true electrode surface areas are proportional to the slopes of plots of  $i_p$  against  $v^{1/2}$ , as shown in Fig. 5. Although Equations 2–4 predict straight lines through the origin, the data shown in Fig. 5 yield slightly positive intercepts. These can be corrected for by baseline subtractions, which presumably take into account factors such as charging current, etc. However, the prediction beforehand of such baseline corrections is somewhat arbitrary and inexact. Providing the baseline corrections are reasonably constant, as the data in Fig. 5 indicate by their excellent linearity, their use is not necessary since only the slope of the plot of  $i_p$  against  $v^{1/2}$  is required to determine the electrode surface area.

Calculations of the roughness factors for the coated and uncoated electrodes are summarized in Table 2. The diffusion coefficient for  $Fe(CN)_6^{3-}$  was taken as  $6.8 \times 10^{-6} \text{ cm}^2 \text{ s}^{-1}$ , which is the value reported by Bazan and Arvia [11] for similar solutions (equimolar  $K_3Fe(CN)_6 + K_4Fe(CN)_6$  (5 mM ~ 10 mM) in 1.0 M NaOH at ~25°C). The value of  $\alpha n_a$  (in Equation 3) was taken as 0.30 for runs with the uncoated electrodes. The close agreement between the roughness factors determined for the gold-coated and uncoated

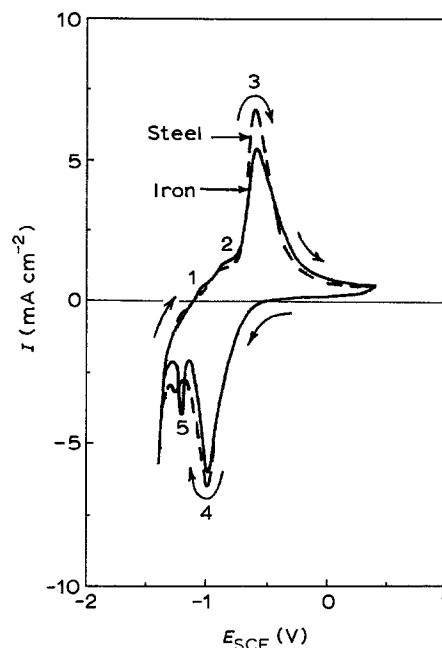


Fig. 6. Comparison of cyclic voltammograms for iron wire and reinforcing steel turnings in cured Portland cement paste, using current densities based on true electrode surface areas. Cell electrolyte was saturated  $Ca(OH)_2$ , water-to-cement ratio = 0.45, 3 day cure, 25°C,  $0.050 \text{ V s}^{-1}$ . Cycle number 201 shown.

electrodes shows that both types of electrodes can be used to determine true surface areas. It is noteworthy that the same value for the relative roughness of the steel (against the iron) was obtained with both gold-coated electrodes and uncoated electrodes (relative roughness = 2.3). However, we have used the roughness factors obtained with the reversible reaction on gold-coated electrodes, since these values are not affected by the additional complexities associated with an irreversible electrode reaction. For example, surface area determinations with a reversible reaction do not require accurate evaluation of the cathodic transfer coefficient ( $\alpha$ ), as is required with irreversible reactions (see Equation 3).

Thus, in order to provide a more representative comparison between the voltammograms for steel and iron shown in Fig. 1, the data of Fig. 1 have been replotted in Fig. 6, using current densities based on the true electrode surface areas (roughness factors of 1.0(6) for the iron electrodes and 2.3(8) for the steel electrodes). The shapes and sizes of the respective voltammograms are very similar; this resemblance is indicative of the similarity of the electrochemical passivation behaviour of iron and steel in cured Portland cement.

Table 2. Calculation of true electrode surface areas and roughness factors\*

	Slope $\times 10^3$ ( $A \text{ V}^{-1/2} \text{ s}^{1/2}$ )	True area ( $\text{cm}^2$ )	Geometric area ( $\text{cm}^2$ )	Roughness factor*
Uncoated steel	0.88	0.206	0.091	2.2(6)
Uncoated iron	0.33	0.077	0.076	1.0(1)
Au-coated steel	1.84	0.262	0.11	2.3(8)
Au-coated iron	1.04	0.148	0.14	1.0(6)

\* Roughness factor = "true" surface area/geometric surface area.

### 3.2. Effects of NaCl and NaNO<sub>2</sub> additions

The effects of NaCl and NaNO<sub>2</sub> additions on the voltammetric behaviour of iron embedded in cement were described in detail in Part II of this study [2]. Significant depassivation of the iron was observed upon potential cycling after exposure to 'external solutions' containing 0.1 M NaCl, and extensive depassivation was observed with 0.2 M NaCl. Admixing 0.6% NaNO<sub>2</sub> prevented depassivation of the iron with up to about 0.4 M NaCl, although film breakdown was observed with 0.6 M NaCl. This depassivation with 0.6 M NaCl was prevented by increasing the amount of NaNO<sub>2</sub> added to the cement from 0.6% to 1.0%. These results were in good agreement with the results of galvanostatic tests reported by Gouda and co-workers [12, 13].

The effects of NaCl and NaNO<sub>2</sub> additions on the voltammetric behaviour of reinforcing steel turnings in cement are shown in Fig. 7 and Table 3 (the current densities are based on the true electrode surface areas). With 0.2 M NaCl in the external solution, but no NaNO<sub>2</sub> admixed, passivity could not be established, as can be seen from the characteristic extremely distorted voltammograms (Fig. 7) and the large current densities flowing in the normally passive region (Table 3). However, upon admixing 0.6% NaNO<sub>2</sub>, the currents in the normally passive region at 0 V decreased by about an order of magnitude (see Table 3), and the voltammograms were much less distorted (Fig. 7). Furthermore, approximately the same level of protection of the reinforcing steel was

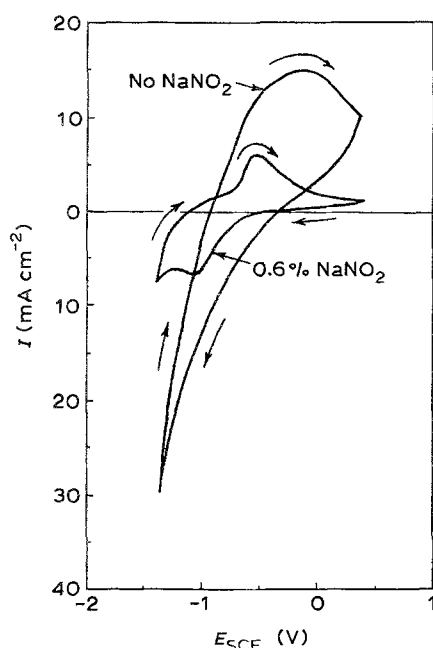


Fig. 7. Cyclic voltammograms for reinforcing steel in cured Portland cement paste with 0.6% NaNO<sub>2</sub> (with respect to the dry cement in the mix) admixed, after exposure for 24 h to an external solution of saturated Ca(OH)<sub>2</sub> + 0.2 M NaCl. Current densities shown are based on the true electrode surface areas. Cycle number 201 shown. Water-to-cement ratio = 0.45, 3 day cure, 25°C, 0.050 V s<sup>-1</sup>.

Table 3. True current densities at 0 V for reinforcing steel and iron in cured cement with and without 0.6% NaNO<sub>2</sub> admixed, and various external NaCl concentrations

[NaCl] (M)	Current density at 0 V (mA cm <sup>-2</sup> )*				
	0	0.1	0.2	0.4	0.6
No NaNO <sub>2</sub>					
Steel	0.7	1.3	15	–	–
Iron	0.8	4.1	16	25	–
0.6% NaNO <sub>2</sub>					
Steel	0.7	1.2	1.7	2.1	13
Iron	0.8	0.8	0.9	1.0	11

\* Current densities are based on true surface areas.

observed with 0.4 M NaCl in the external solution as with 0.2 M NaCl, although much greater voltammetric current densities were observed with 0.6 M NaCl in the external solution. Thus, the results shown in Table 3 clearly show that the trends and conclusions obtained with reinforcing steel embedded in salt-contaminated cement, both with and without 0.6% admixed NaNO<sub>2</sub>, are basically the same as those obtained for embedded iron.

### 4. Concluding remarks

The similarity of the voltammetric behaviour of both reinforcing steel and iron in cement, with and without NaCl and NaNO<sub>2</sub> additions, confirms that the results and conclusions obtained using iron wire in the voltammetric method described in previous communications [1, 2] are also applicable to the behaviour of reinforcing steel.

### Acknowledgement

The financial support of the Natural Sciences and Engineering Research Council of Canada is gratefully acknowledged.

### References

- [1] J. T. Hinatsu, W. F. Graydon and F. R. Foulkes, *J. Appl. Electrochem.* **19** (1989) 868.
- [2] *Idem, ibid.* **20** (1990) 841.
- [3] V. K. Gouda and M. K. Shater, *Corros. Sci.* **15** (1975) 199.
- [4] J. B. Vrable and B. E. Wilde, *Corrosion* **36** (1980) 18.
- [5] J. A. Gonzalez and C. Andrade, *Br. Corros. J.* **17** (1982) 21.
- [6] B. W. Cherry and A. S. Kashmirian, *ibid.* **18** (1983) 194.
- [7] H. H. Uhlig, 'Corrosion and Corrosion Control', 2nd ed. John Wiley & Sons, New York (1971).
- [8] G. J. Verbeck, in 'Corrosion of Metals in Concrete', ACI SP-49-3, ACI, Detroit (1975) pp. 21–38.
- [9] D. W. Kirk, F. R. Foulkes and W. F. Graydon, *J. Electrochem. Soc.* **125** (1978) 1436.
- [10] A. J. Bard and L. R. Faulkner, 'Electrochemical Methods', John Wiley & Sons, New York (1981) pp. 218–23.
- [11] J. C. Bazan and A. J. Arvia, *Electrochim. Acta* **10** (1965) 1025.
- [12] V. K. Gouda and G. E. Monfore, *J. Res. Dev. Labs Portl. Cement Assoc.* **7**(3) (1964) 24.
- [13] V. K. Gouda and W. Y. Halaka, *Br. Corros. J.* **5** (1970) 204.